International Journal of Engineering, Science and Mathematics
Vol. 7 Issue 3, March 2018,
ISSN: 2320-0294 Impact Factor: 6.765
Journal Homepage: http://www.ijesm.co.in, Email: ijesmj@gmail.com
Double-Blind Peer Reviewed Refereed Open Access International Journal - Included in the International Serial Directories Indexed & Listed at: Ulrich's Periodicals Directory ©, U.S.A., Open J-Gage as well as in Cabell's Directories of Publishing Opportunities, U.S.A

THE HYDRODYNAMICS OF CAPILLARY RISE USING NEUMERICAL METHOD

Mahesh Kumar[1], Dr. Ajay Singh[2]

Department of Physics

Chaudhary Charan Singh University, Meerut

Abstract

The capillary rise phenomena have many applications in diverse areas, such as civil engineering, oil recovery, textile, and others. Researchers' research therefore has always been in the both theoretical as well as functional aspect of capillary rise hydrodynamics. In this research its hydrodynamic degree was studied for simulations on two and single-phase fluids using the lattice-Boltzmann method. The goal of such analysis regarding simulations was to properly established the relation between the wetting i.e. solid-liquid as well as the gas-liquid (surface tension). It is this analysis that we see how much the lattice-Boltzmann method has the advantage of simulating regarding the very well familiar capillary rise phenomena, and thus system was evaluated in a narrow capillary pipe on to an uprising fluid.

I INTRODUCTION

Many natural forces and anthropogenic impacts are highly dependent upon on capillary effect , i.e. the potential of liquids to penetrate the wettable walls via finer pores and cracks, and also to be extracted from those with unweathered walls. That is the capillarity which brings water to the upper layer of soil, moves sap in plants and paves the way for the operation of the pens. Awareness of capillarity laws is applicable in the fields of oil extraction, civil engineering, textile fabric dyeing, ink printing and many others. This demonstrates the growing interest in the subject from industry and basic science. Therefore the capillary rise phenomena seems to be of broad practical and theoretical attention in recent years (1-5), with implementations extended from basic capillary rise as well as imbibition (insertion of liquid in droplet form into porous material) up tothe droplet spread as well as other wetting-related phenomena. Major theories related with analytical studies for capillary rise have been established very earlier (6), but latest analytical and simulation techniques gave unique perspective into to this issue: the first lattice-gas automation models (7-11) upon this

International Journal of Engineering, Science and Mathematics
Vol. 7 Issue 3, March 2018,
ISSN: 2320-0294 Impact Factor: 6.765
Journal Homepage: http://www.ijesm.co.in, Email: ijesmj@gmail.com
Double-Blind Peer Reviewed Refereed Open Access International Journal - Included in the International Serial Directories Indexed & Listed at: Ulrich's Periodicals Directory ©, U.S.A., Open J-Gage as well as in Cabell's Directories of Publishing Opportunities, U.S.A

numerical side, and now the lattice-Boltzmann methods (10, 12-14). Now there are manypaths to introduce interactions amongst fluid's particles and also between particles of fluid with the environment (15–22), and also the methods have also been verified experimentally, particularly in the form of particle suspension (23) and flow in complicated geometrical (24–26).

We recognize capillary phenomenon in the current study and are proposing a model for them. After introduction firstly, we describe the theoretical hydrodynamic structure briefly in Section 2, to which we will relate our results and provide detailed technical information of simulations. Section 3 describes the findings while Section 4 and Section 5 provide review and conclusion.

II CAPILLARY PHENOMENON AND STIMULATION MODEL

Naturally, the most simple example regarding capillary phenomenon is the growth in term of fluid' level inside the capillary-tube, and this process has an critical role especially as liquid's dropletenters theporous content. Since capillary-rise theory is well developed, it provides a benchmark testregarding the methods which are used for simulate imbibition into the porous media. As perWashburn's classical review (27), fluid which is incompressible viewed as a Poiseuille's flow (28). Considering the upward increase of liquid (incompressible) inside a capillary pipe, a start can be consider from the equation of Hagen-Poiseuille for a formed pipe flow at ΔP(change in pressure) during drop,

$$\frac{dQ}{dt} = \frac{\pi \Delta P r^4}{8\mu_f (h + h_+)}, \qquad (1)$$

In equation, volumetric flow rate is$dQ/dt = \pi r^2 dh/dt$;h = liquid column's heightwhich is rising w.r.t. liquid surface's leveloutside pipe whileh_+= immersed capillary pipelengthinside liquid,μ_f =liquid viscosity and r = pipe radius.

Overall decrease in pressure is expressed as capillary pressure + the static pressure exerted due to gravity:

$$\Delta P = \frac{2\gamma \cos\theta_d}{r} - \rho_f g h, \qquad (2)$$

International Journal of Engineering, Science and Mathematics
Vol. 7 Issue 3, March 2018,
ISSN: 2320-0294 Impact Factor: 6.765
Journal Homepage: http://www.ijesm.co.in, Email: ijesmj@gmail.com
Double-Blind Peer Reviewed Refereed Open Access International Journal - Included in the International Serial Directories Indexed & Listed at: Ulrich's Periodicals Directory ©, U.S.A., Open J-Gage as well as in Cabell's Directories of Publishing Opportunities, U.S.A

Where γ = surface tension; θ_d= dynamic contact angle and ρ_f = fluid density. The contact angle is constant in classical capillary rise theory, but in phenomenologicallyrevised fashion (27) of this theory. As the contact angle changesalong velocity thus it is called dynamic contact angle. And by combining the eq. (1) and (2), eq. (3) mention below was obtained.

$$8\mu_f(h+h_+)\frac{dh}{dt} = 2r\gamma\cos\theta_d - r^2\rho_f gh\,. \quad (3)$$

By adding both entrance as well as inertial effects (28), and by terms rearranging, eq. (3) becomes

$$\cos\theta_d = \frac{1}{2\gamma}\left(\rho_f rh\frac{d^2h}{dt^2} + \frac{8\mu_f(h+h_+)}{r}\frac{dh}{dt} + \frac{1}{4}\rho_f r(\frac{dh}{dt})^2 + \rho_f rgh\right). \quad (4)$$

Eq. (3) is Washburn equation. This is used to compare height of simulated column with dynamic contact angle.

Inertial forces are ignored in our system's overdamped limit (29), to metvariable values. Asymptotically, at long times(t=∞), we get eq (5) when dh/dt=0,

$$h_\infty = \frac{2\gamma\cos\theta_\infty}{\rho_f gr}, \quad (5) \quad \text{Where} \quad \theta_\infty = \lim_{t\to\infty}\theta_d\,.$$

Because of the irregeular discretization as well as the sharp density variance, perticularly for radius r, measurement ofθ_d accurately via simulated density field is difficult. For determination (indirect) of θ_d, we 1st apply the 1-D Reynolds transport theorem for control volume so that the rate of change for device momentum can be estimated. Upper control surface shifts with liquid column's meniscus (no control-volume outflow) as well as the lower surface of control at lower pipe endis fixed. Then rate of total momentum change within the control volume is –

$$\frac{d}{dt}(m\mathbf{v})_{syst} = \frac{d}{dt}[\int_{CV}\mathbf{v}\rho dV] + \int_{CS}\mathbf{v}\rho(\mathbf{v}\cdot\mathbf{n})dA, \quad (6)$$

International Journal of Engineering, Science and Mathematics
Vol. 7 Issue 3, March 2018,
ISSN: 2320-0294 Impact Factor: 6.765
Journal Homepage: http://www.ijesm.co.in, Email: ijesmj@gmail.com
Double-Blind Peer Reviewed Refereed Open Access International Journal - Included in the International Serial Directories Indexed & Listed at: Ulrich's Periodicals Directory ©, U.S.A., Open J-Gage as well as in Cabell's Directories of Publishing Opportunities, U.S.A

Where total fluid mass inside the control volume = m=m(t);fluid's velocity of control volume =*CV*and controlvolumes surface area = *CS*. After integration eq (7) we get as follows-

$$\frac{\mathrm{d}}{\mathrm{d}t}[\int_{cv}\mathbf{v}\rho_f \mathrm{d}V] = \rho_f \pi r^2\left(h\frac{\mathrm{d}\mathbf{v}}{\mathrm{d}t}+\mathbf{v}\frac{\mathrm{d}h}{\mathrm{d}t}\right)=\frac{\mathrm{d}(m\mathbf{v})_{cv}}{\mathrm{d}t}, \qquad (7)$$
$$\int_{cs}\mathbf{v}\rho(\mathbf{v}\cdot\mathbf{n})\mathrm{d}A = -\mathbf{v}(\rho_f \pi r^2 v).$$

Where v = liquid's velocity while n = unit vector normal to the inlet controlsurface. By assuming constant velocity over the control surface, wegeta new eq for$\theta_d$byplacingeq. (4) into eqs. (6) and (7),

$$\cos\theta_d = \frac{1}{2\pi r\gamma}[\frac{\mathrm{d}(mv)_{cv}}{\mathrm{d}t}-\frac{3}{4}\rho_f \pi r^2 v^2 + 8\pi\mu_f(h+h_+)v+\rho_f \pi r^2 gh]. \qquad (8)$$

Equation (8), a right form in Ref. (12), determine $\theta_d$via simulated h(t). The results, however, remain same, particularly for long times, as the speed of rise is less. The position of gas-liquid interface or column height h(t) determined bydensity profile's function in vertical direction as a turning point of the least-squares fit.

It addressed a variety of empirical associations for wetting content, describing the dynamic contactangle θ_d as capillary number's function Ca = vμ/π during spreading so that the advancing contact angle θa is the liquid spreadingat the $v \to 0^+$limit.
We used the term widely accepted instudies (29) regarding capillary-rise,

$$\cos\theta_d = \cos\theta_a - A\mathrm{Ca}^B, \qquad (9)$$

In above eq*A* as well as *B* are constants. Bysimulations, the dependence on $\theta_a$and Caof $\theta_d$was tested, by which between them above relation was found.

International Journal of Engineering, Science and Mathematics
Vol. 7 Issue 3, March 2018,
ISSN: 2320-0294 Impact Factor: 6.765
Journal Homepage: http://www.ijesm.co.in, Email: ijesmj@gmail.com
Double-Blind Peer Reviewed Refereed Open Access International Journal - Included in the International Serial Directories Indexed & Listed at: Ulrich's Periodicals Directory ©, U.S.A., Open J-Gage as well as in Cabell's Directories of Publishing Opportunities, U.S.A

III RESULT

The following simulations were reported for radii of pipe r = 2, 5 and 10 while the maximum domain size was 50x50x50, and 100x100x300 for pipe radii r = 20. The relaxation parameter in all capillary rise, τ =1 was simulations, unless specified, the adhesive variables were G = -0.15 and W = -0.1. This culminated in $\rho_f / \rho_g \approx 20$, with the bulk density ρ_f = 2.25, surface tension γ = 0.085and viscosity μ_f = 0.375 of liquid phase. For the presentation of the results in dimensionless units, the dimensional analysis was done for the variables (g, ρ_f, h, t, μ_f and γ) group. Accordingly, we defined the characteristic time = $t_0 = \mu^3_f / \rho_f\gamma^2 \approx 3.2$, velocity = $v_0 = \gamma / \mu_f \approx 0.23$ and height $h_0 = \mu^2_f / \rho_f\gamma \approx 0.74$. And inthe presence of gravity a dimensionless variableg $=\mu^4_f g/ \rho_f\gamma^3$is used.

Figure 1 of the pipes having different radii velocity profile, and compared them with the White's analytical results (28). This velocity profile calculated from a constant flow of two- or single-phase fluid between 2 infinite parallel platesat its equilibrium density and constant body forcereagrding each lattice point, created the flow in the 2-phase modelwithout any phase separation. In figure 2, of the density profile, there was no bulk density of liquid anywhere in narrow pipe with radius r = 2. However, for radius r = 5, 10 and 20, at poor adhesion forces, such as W = to -0.1, the decay regarding density near the inside of pipe walls was compared. With decreasing radius, thebulk density also decreased the same proportion for liquid. We found that the velocity profile (simulated) reached towards the theoretical curve to increase adhesion, and in the density profile boundary effects decreased (as seen in the curves for radius r = 20 as seen in Figure 2). The fluid'sdensity in the 1st layer which is next to the wall has increased with the adhesion (not shown), but the extent of the effect was similar on the wall (liquid layer having thickness of aboutsome spacing in lattice) density. In 3 and 4 figures,the dynamic touch angle and the height of the column are represented as simulation time functions for radius r = 5 and 20. Our result also displayed the findings, with and without the influence of gravity, for comparison while maintaining contant W = -0.1. The capillaryrise velocity with period for both null- and non-zero-gravity is in Figure 5. The first column accelerated rapidly, and approximately $t^{1/3}$ then decayed to stationary state. However it takes time and simulating more to correctly adjust the exponent. The acceleration was the

result of the pipe being rapidly inserted into the device; decline in non-zero gravity velocity was almost completely independent from radius of capillary.

IVDISCUSSION

We initially modelleda 3-D,2-phase fluid system using the lattice-Boltzmann method (12), with periodic lateral boundaries and no pipes. The simulation code wasalready checked for flow through porous media,single-phase fluid and several benchmark results of different studies (30). After a certain number of iterations, the pipe was inserted when the system entered the equilibrium state and the simulation proceeded until the capillary increase was saturated (cf. the snapshots in the Figures 3 and 4 insets for r=5 and 20, respectively). A significant question is about the variance in the radius of capillary in the 2-phase flow model affects the dynamics of the flow. We measured the velocity profile for pipes with different radii to answer this question and correlated it with the analytical results (12) (see Figure 1). In Figure 1 the complete lines also display the velocity profile and analytical results for Poiseuille flow (12). A comparison of analytical results suggested that the velocity profile in stimulation resultsof this study had the right parabolic shape (Poiseuille). This relative variance increased for the boundary effects as decrease in radius was predicted. Strong boundary-layer influence was the explanation for this deviation. The adhesive force described in the 2-phase lattice-Boltzmann model equation and produces a low density liquid layer on pipe's surface. We not expect great results for pipe having radius r = 2, due to very low resolution, and for strong adhesion both radius 5 and 10 were very weak as seen figure 2 for density profile.Column height was decrease in as suggested from eq (3) with increase in pipe size. Without gravity, as eq (3) would have predicted, the column grew more rapidly with increasing radius of the shaft. In addition, there was an increase in column height, which is supposed to increase pipe size. The strong lines in Figures 3 and 4 indicate eq (4)'s respective numerical solutions, where eq (8) determined the complex contact angle θd.If the contact angle was maintained fixed, a reasonable agreement could only be achieved between the Washburn equation as well as the simulation data for a short time window up to $t / t / \approx$ 1000.By using θd in the Washburn equation from eq. (8), there was strong agreement was found for large radius to the last data points where due to increase in interface velocity some

International Journal of Engineering, Science and Mathematics
Vol. 7 Issue 3, March 2018,
ISSN: 2320-0294 Impact Factor: 6.765
Journal Homepage: http://www.ijesm.co.in, Email: ijesmj@gmail.com
Double-Blind Peer Reviewed Refereed Open Access International Journal - Included in the International Serial Directories Indexed & Listed at: Ulrich's Periodicals Directory ©, U.S.A., Open J-Gage as well as in Cabell's Directories of Publishing Opportunities, U.S.A

variance occurred near the end of the pipe. At the start of simulations, which can be seen in figure 3 and figure 4, we had $\cos\theta d = 0$, or $\theta d = \pi/2$.After that the contact angle θd associated with Ca decreased or decreased with rising time. The steady state contact angle was quickly reached in a few 100 time steps from the total simulation time (about fifty thoudand time steps) particularly in the presence of gravity. Rising of cosθd at limited scale this resulted the liquid is hitting the pipe end. For long periods and small capillary numbers which mean slow interface speeds, a constant as expected has been approached by θd.An improvement in steady state contact angle for raising the pipe length, is unphysical and it is because of the complexity of calculating the exact angle from simulation data. The relative value of the other resistive forces in eq (4)for stronger gravity, a decline and a more stable behaviour of θd was more consistent. This supports the notion that our simulation model has very different frictional forces from those assumed in the hydrodynamic derivation of eq. (8).

V CONCLUSION

The capillary rise phenomenon can alsobe studied by lattice-Boltzmann method numerically, at the level of hydrodynamic. However, for practical kinetics due to discrete effects one requires very thick (in lattice units) tubing. The pipe diameter should be at least 30 lattice units, for the parametrization used here. Future work involves validation or alteration of the velocity profile (theoretical) at walls of a narrow capillary having strong adhesive forces. Somewhat thinner pipes are suitable for the static or unchangeableproperties in of gravity's presence, whereas thicker pipes are required in the case of strong adhesion.

References: -

1. S.A. Safran, Statistical Thermodynamics of Surfaces, Interfaces and Membranes *(*AddisonWesley, Reading, 1994).
2. L.H. Tanner, J. Phys. D: Appl. Phys. 12, 1473 (1979).
3. M. Pasandideh-fard, Y.M. Qiao, S. Chandra and J. Mostaghimi, Phys. Fluids 8, 650 (1996).
4. C. Treviño, C. Ferro-Fontán and F. Méndez, Phys. Rev. E 58, 4478 (1998).
5. S. Betelú, B.M. Law and C.C. Huang, Phys. Rev. E 59, 6699 (1999).
6. M. Dubé, M. Rost and M. Alava, Europhys. J. B **15**, 691 (2000), and references therein.
7. *Lattice gas methods for partial differential equations*, edited by G.D. Doolen*(Addison-Wesley,Redwood City, CA, 1990).*
8. S. Chen and G.D. Doolen, Annu. Rev. Fluid Mech. **30,** 329 (1998).
9. U. Frisch, D. d'Humières, B. Hasslacher, Lallemand, Y. Pomeau and J-P. Rivet, Complex
   Systems **1**, 649 (1987).
10. D.H. Rothman, J. Geophys. Research **95**, 8663 (1990).
11. V. Pot, C. Appert, A. Melayah, D.H. Rothman and S. Zaleski, J. Phys. II **6**, 1517 (1996).
12. P. Raiskinmäki, A. Shakib-Manesh, A. Koponen, A. Jäsberg, J. Merikoski and J. Timonen,
    Lattice-Boltzmann simulation of capillary rise dynamics, J. Stat. Phys. **107**, 147 (2002).
13. X. He and L.S. Luo, Phys. Rev. E **56**, 6811 (1997).
14. A.K. Gunstensen, D.H. Rothman, S. Zaleski and G. Zanetti, Phys. Rev. A **43**, 4320 (1991).
15. A. K. Gunstensen, D. H. Rothman, S. Zaleski, and G. Zanetti, Phys. Rev. A 43:4320 (1991).
16. A. K. Gunstensen and D. H. Rothman, Europhys. Lett. 18:157 (1992).
17. N. S. Martys and H. Chen, Phys. Rev. E 53:743 (1996).
18. X. Shan and H. Chen, Phys. Rev. E 47:1815 (1993).
19. X. Shan and H. Chen, Phys. Rev. E 49:2941 (1994).
20. E. Orlandini, M. R. Swift, and J. M. Yeomans, Europhys. Lett. 32:463 (1995).
21. M. R. Swift, E. Orlandini, W. R. Osborn, and J. M. Yeomans, Phys. Rev. E 54:5041 (1996).
22. G. Gonnella, E. Orlandini, and J. M. Yeomans, Phys. Rev. E 58:480 (1998).
23. A. J. C. Ladd, J. Fluid. Mech. 271, 285 (1994); ibid. 271, 311 (1994); A. J. C. Ladd and R. Verberg, J. Statist. Phys. 104, 1191 (2001).

24. A. Koponen, D. Kandhai, E. Hellén, M. Alava, A. Hoekstra, M. Kataja, K. Niskanen, P. Sloot, and J. Timonen, Phys. Rev. Lett. 80:716 (1998).
25. B. Ferre`ol and D. H. Rothman, Transport in Porous Media 20:3 (1995).
26. P. Raiskinmäki, A. Koponen, J. Merikoski, and J. Timonen, Comp. Mat. Sci. 18:7 (2000).
27. E.W. Washburn, Phys. Rev. 17, 273 (1921).
28. F.M. White, Fluid Mechanics (McGraw Hill, New York, 1993).
29. E. Schäffer and P. Wong, Phys. Rev. E 61, 5257 (2000).
30. A.I. Koponen, Simulation of fluid flow in porous media by lattice gas and lattice Boltzmann methods, PhD thesis, *University of Jyväskylä*(1998).

List of Figures: -

Figure no. 1. A typical example of the velocity profile of the fully developed flow of a single-phase (W = G = g = 0) fluid, and of a two-phase (W = -0.1, G = -0.15, g = 0) fluid, between two parallel plates.

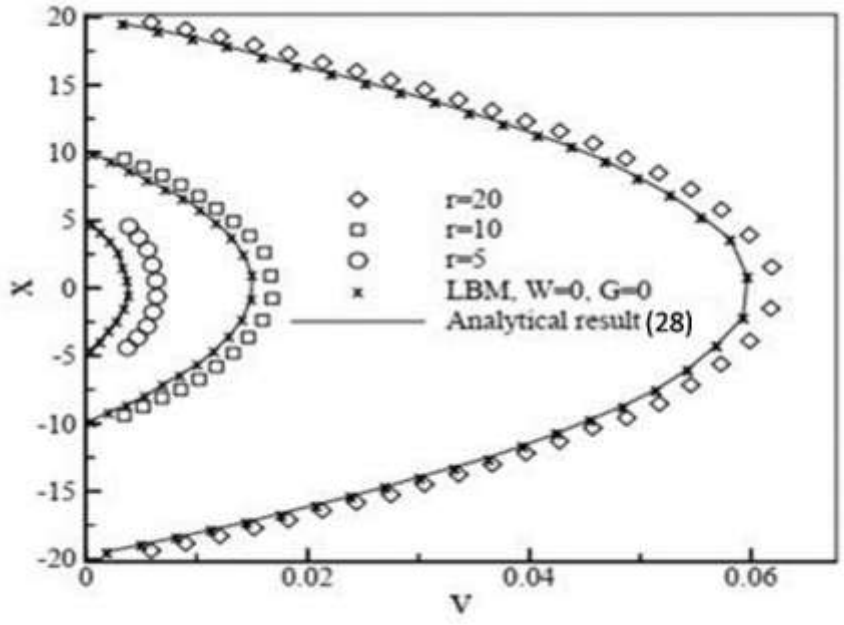

Figure no. 2. The density profiles across the capillary pipe for radii r = 2, 5, 10 and 20 as functions of distance from the centerline of the pipe.

International Journal of Engineering, Science and Mathematics
Vol. 7 Issue 3, March 2018,
ISSN: 2320-0294 Impact Factor: 6.765
Journal Homepage: http://www.ijesm.co.in, Email: ijesmj@gmail.com
Double-Blind Peer Reviewed Refereed Open Access International Journal - Included in the International Serial Directories Indexed & Listed at: Ulrich's Periodicals Directory ©, U.S.A., Open J-Gage as well as in Cabell's Directories of Publishing Opportunities, U.S.A

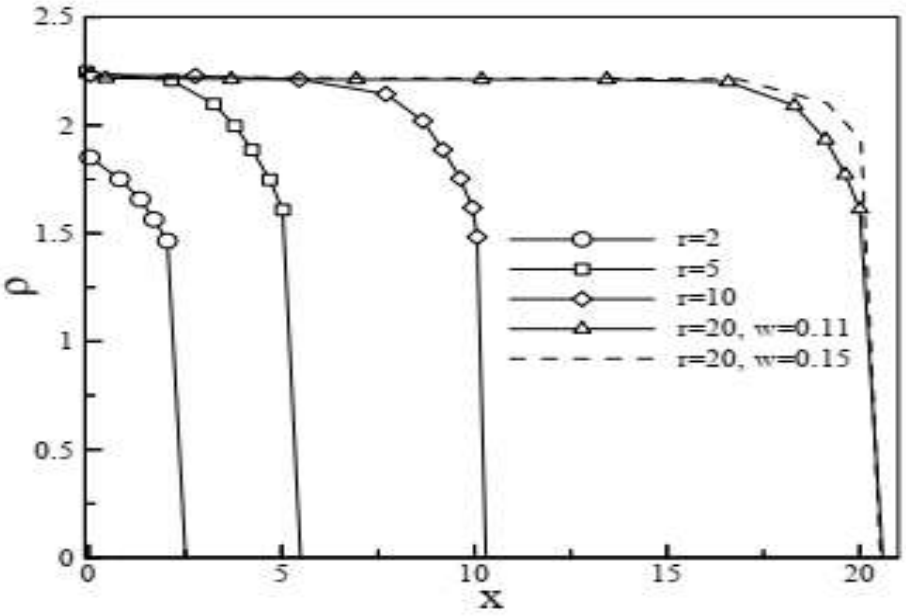

Figure no. 3. The height of the column and the dynamic contact angle as functions of simulation time for the pipe radius r = 5. The inset shows three snapshots of the capillary rise: initial, intermediate, and steady state (side view).

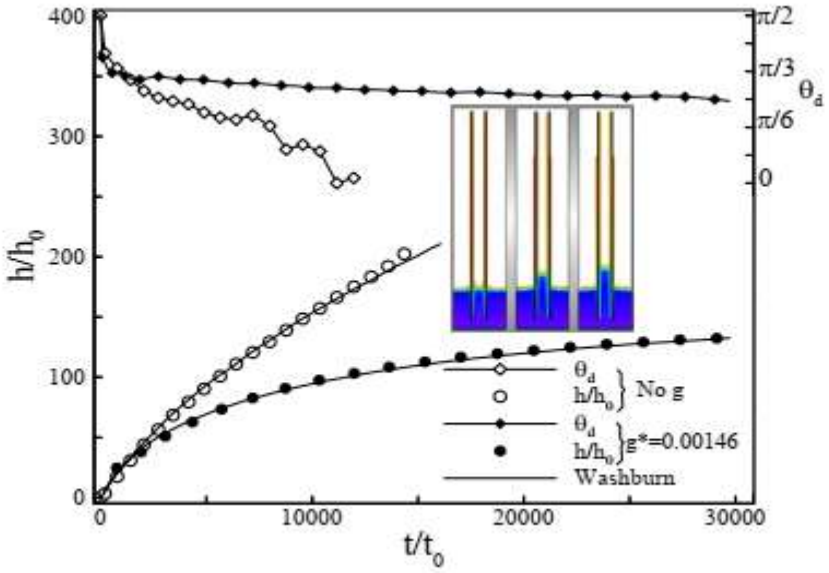

Figure no. 4. The height of the column and the dynamic contact angle as functions of simulation time for the pipe radius r = 20. The inset shows three snapshots of the capillary rise: initial, intermediate, and steady state (side view).

International Journal of Engineering, Science and Mathematics
Vol. 7 Issue 3, March 2018,
ISSN: 2320-0294 Impact Factor: 6.765
Journal Homepage: http://www.ijesm.co.in, Email: ijesmj@gmail.com
Double-Blind Peer Reviewed Refereed Open Access International Journal - Included in the International Serial Directories Indexed & Listed at: Ulrich's Periodicals Directory ©, U.S.A., Open J-Gage as well as in Cabell's Directories of Publishing Opportunities, U.S.A

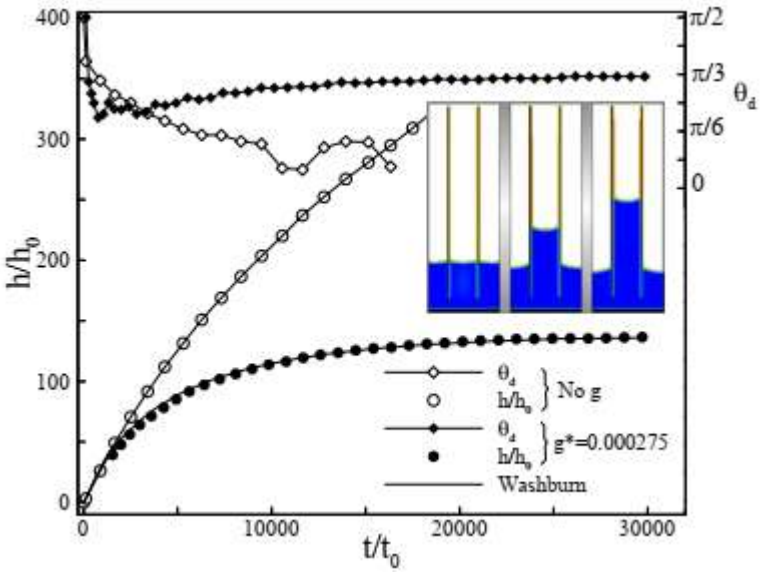

Figure no. 5. Normalized velocity of the column as a function of simulation time.